Tikrit Journal of Engineering Sciences

TJES Tikrit Journal of Engineering Sciences

Open Access

Article

Removal of Methylene Blue Dye from Wastewater Using a Local Iraqi Natural Plant Polypogon Monspeliensis

Hind A. Ahmed [1], Hiba B. Deab [2], Alaa E. Sultan [2], Peter Oladoye [3], Hawraa R. Bohan [4], Mohammed Kadhom [1]*

[1] Department of Environmental Science, College of Energy and Environmental Science, Alkarkh University of Science, Baghdad, 10081, Iraq.
[2] Department of Chemistry, College of Science, University of Diyala, Baquba, 32001, Diyala, Iraq.
[3] Department of Chemistry and Biochemistry, Florida International University, Miami, 33199, Florida, United States.
[4] Central Environmental Laboratory, Ministry of Environment, Baghdad, 10044, Iraq.

Emails:
Hind A. Ahmed: hind.ahmed@kus.edu.iq , Hiba B. Deab: hibabassem4@gmail.com , Alaa E. Sultan: alaesa1988@gmail.com ,
Peter Oladoye: polad001@fiu.edu , Hawraa R. Bohan: H.bohan0911@coeng.uobaghdad.edu.iq , Mohammed Kadhom: kadhom@kus.edu.iq

Abstract:

The present work investigated the use of Polypogon monspeliensis (PM) as an environmentally friendly and economical adsorbent for the removal of methylene blue (MB) from simulated wastewater. Both batch and column adsorption experiments were carried out to examine the adsorption performance under different operational conditions. Structural and chemical characterization of the adsorbent was conducted before and after adsorption using X-ray diffraction (XRD) and Fourier transform infrared (FTIR) spectroscopy. In batch studies, factors of pH, adsorbent dosage, dye concentration, contact time, and temperature were applied to evaluate the impact on the removal efficiency. Furthermore, kinetics, isotherms, and thermodynamic studies were conducted to understand the adsorption mechanism. On the other side, a fixed bed column setup was employed to investigate PM's performance in continuous mode adsorption. Results indicated that PM exhibited high efficiency in MB removal, with removal rates exceeding 80% across the conditions studied. Optimal conditions were identified to be neutral pH, moderate (0.5 g/50 ml) adsorbent dosage, low initial dye concentrations, and 30 min time. The maximum adsorption capacity is 20.2 mg/g. The kinetics of the process also show that it is a pseudo-second-order rate process, indicating chemisorption as the main mechanism of removal. The results from the isotherm also show that chemisorption is the main mechanism of MB removal, as the Langmuir and Freundlich models gave a good fit to the results. The thermodynamics of the process show that it is a spontaneous, endothermic process with increasing interface randomness with increasing temperature. In continuous-mode adsorption, PM effectively removed MB, with removal rates influenced by flow rate, initial concentration, and column height. These findings showed effective MB removal for up to 90 min; the removal rates were maintained at 96% and 94% when column heights of 10 cm and 5 cm were used, respectively, at a flow rate of 75 ml/min and a dye concentration of 20 ppm.

Keywords:

Methylene blue; Polypogon monspeliensis; Adsorption; Water treatment; Biowaste.

Highlights:

- Study explores Polypogon monspeliensis for methylene blue adsorption.
- Batch and continuous systems optimize PM's efficiency, achieving >80%.
- Optimal conditions identified: neutral pH, moderate dosage, low dye concentration, and 30 min contact time.
- Adsorption kinetics reveal a pseudo-second-order mechanism, supported by Langmuir and Freundlich isotherms.
- Thermodynamic analysis indicates a spontaneous and endothermic process, with increased unpredictability at higher temps.

Citation:

Ahmed HA, Deab HB, Sultan AE, Oladoye P, Bohan HR, Kadhom M. **Removal of Methylene Blue Dye from Wastewater Using a Local Iraqi Natural Plant Polypogon Monspeliensis**. *Tikrit Journal of Engineering Sciences* 2026; **33**(1): 2044.

Article History:

Received:	05	Mar.	2024
Received in revised form:	03	Aug.	2024
Accepted:	16	Mar.	2024
Final Proofreading:	16	Mar.	2026
Available online:	14	May	2026

https://doi.org/10.25130/tjes.33.1.24

Corresponding Author*:

Mohammed Kadhom
Department of Environmental Science, College of Energy and Environmental Science, Alkarkh University of Science, Baghdad, 10081, Iraq.
Email: kadhom@kus.edu.iq

1.INTRODUCTION

Globally, 2.2 billion people lack access to clean water, while 800 million lack basic drinking water because of scarce water resources [1]. In addition, water resources are being overused. The Southeast Asian region is becoming increasingly vulnerable to water shortages due to climate change [2]. The water resources of the Middle East and North Africa (MENA) will be affected by climate change, population increase, economic development, and environmental factors [2, 3]. By using highly sophisticated hydrological modeling techniques, water allocation modeling, and a two-step approach, it has been predicted that with an average climate change scenario, the total water demand of MENA will be 393 km^3 per year by 2050 [4]. There will be a shortage of 199 km^3 per year. This increase will be due to a 12% fall in supply and a 50% increase in demand. The predicted water shortage will vary between 85 and 283 km^3 per year by 2050. This has been calculated using nine General Circulation Models. The shortage will be due to 78% changes in socioeconomic factors and 22% due to climate change [3]. There are three main types of dyes: anionic, cationic, and nonionic. Each type has its own set of dyes. There are three types of anionic dyes: direct, reactive, and acid dyes. There are also two types of cationic and nonionic dyes: basic and diffused dyes, respectively [4]. Methylene blue (MB) is used a lot in the chemical, medical, and biological fields, as well as in the clothing industry. It has a complicated structure and a positive charge, which makes it hard to get rid of [5]. Methyl orange (MO) is also used in many different fields and has a molecular weight that is similar to that of MB [6]. Methyl red, an azo dye with a high molecular weight, is also hard to get rid of, along with methyl orange. There are also other acidic and basic dyes that need to be thrown away. Treating dye-polluted water may represent a source of pure water that contributes to fulfilling the global need. Various techniques, including filtration, chemical oxidation, coagulation, electrochemical removal, photocatalysis, ultrasonic and biological breakdown, and adsorption, are employed to purify water contaminated with dyes [7, 8]. Adsorption, particularly advantageous for its ease of use, high efficiency, and lack of toxic byproducts, involves the binding of certain chemicals or ions to the surfaces of a solid material called an adsorbent. Over the years, various materials have served as adsorbents for diverse chemicals [9, 10]. In addition to its simplicity, usability, effectiveness, affordability, renewability, and minimal environmental impact, adsorption is notably more cost-effective, ranging from $5 to $200/$m^3$, compared to alternative water purification methods costing between $10 and $450/$m^3$ [11, 12]. After evaluating the pros and cons of different methods, research teams extensively scrutinize adsorption as the most advantageous option [13]. There has been a notable focus in recent years on using biomass waste, namely agricultural waste, to remove stains. This waste is produced in substantial volumes as a result of the growing food business linked to the rising world population. Hence, biowaste is a great resource for producing adsorbents because of its cost-effectiveness, extensive availability (since it is produced in all inhabited places worldwide), and proven effectiveness. The integration of this resource in the adsorption process entails either the immediate consumption or the creation, operation, and/or production of adsorbents [14]. Thermal treatment has been used to manufacture nanomaterials from several types of agricultural waste, including peels, leaves, seeds, and so on [15]. Portions of these materials have also been exploited, and in several cases, they have been directly employed without additional processing. The utilization of biowaste was intensively investigated by many groups, including ours. However, natural plants represent another source of bio-based adsorbents that were not widely considered for wastewater treatment. They grow in almost all places and most of them are seasonal; after the planting season ends, they dry and die, leaving a body that may be used as an adsorbent. These plants are classified into many families, where some are investigated and others are not. They are a free and abundant source of different types of adsorbents if they perform well for this purpose. In a recent study by Duan et al., the natural plant Angelica Sinensis (AS) underwent a straightforward alkaline-heat treatment, leading to a product used to prepare a stable foam [16]. The positive impact of cellulose dissociation and the conversion of ligustilide into amphiphilic molecules on enhancing the stability of Pickering foam was revealed. The liquid foam served as a pore-foaming template and a precursor for polymerization, allowing the synthesis of a porous adsorbent through a one-step integrated process involving free radical polymerization and silane hydrolysis. The resulting porous adsorbent exhibited a well-defined porous structure and exceptional adsorption performance for cationic dyes. Maximum adsorption capacities of 386.13 mg g^{-1} and 284.20 mg g^{-1} are achieved for methyl violet (MV) and malachite green (MG), respectively. The same group reported the use of the prepared foam in removing Cd^{2+} and Cu^{2+} ions from wastewater [17]. Here, the adsorption capacities for Cd^{2+} and Cu^{2+} reached 372.74 mg/g and 186.83 mg/g, respectively. Also, several biopolymers (chitosan, collagen, cellulose, starch, pectin, lignin, and alginate) and natural gums (guar, gellan, carrageenan, karaya, moringa oleifera, tragacanth, and

xanthan gum) were applied in adsorption. These composites are not poisonous, economically feasible, environmentally sustainable, and own outstanding surface functionality. For instance, Starch-based composites have been effectively created to treat wastewater by capturing dyes. More precisely, the utilization of magnetic carbonaceous maize starch, which is an economical biopolymer, has demonstrated high effectiveness in eliminating Methylene Violet (MV) dye. The adsorption process was determined to be both endothermic and spontaneous. Notably, the adsorbent exhibited the capacity to be regenerated for a maximum of six cycles [18]. The last example of using natural plants for water purification is the use of Hibiscus rosa-sinensis for eliminating MB dye from water. Through a series of systematic tests, important factors such as the initial dye concentration, contact time, and pH were adjusted in order to optimize the adsorbent's efficiency. The decolorization efficiency was particularly remarkable, reaching an astonishing 86% for a dye concentration of 10 mg L^{-1} at a pH of 6 [19]. In this work, Polypogon monspeliensis (locally called Shikh Esmallah) was used to adsorb MB from simulated wastewater in batch and continuous systems. Different operation conditions and characterization techniques were applied to identify the optimum conditions and the performance of the plant. This plant presented very high results compared with its simple use, where the removal rate exceeded 80% in all studied factors. This project motivated our group to study this plant intensively in our upcoming project.

2.MATERIALS AND METHODS

2.1.Chemicals and Characterization Techniques

In this work, Polypogon monspeliensis (PM) was collected from the gardens of Alkarkh University of Science at Abu Ghraib/Baghdad, where its inflorescence was utilized for adsorption. MB of a molecular weight of 319.86 g/mol and a chemical structure of $C_{16}H_{18}ClN_3S$ xH_2O was purchased from R&M Chemicals, India. Distilled water was employed for formulating the dye solutions throughout the research. Sodium hydroxide (NaOH) and hydrochloric acid (HCl, 37%) were also purchased from R&M Chemicals. The dye solution was centrifuged using a PLC-03-GEMMY centrifuge device from Taiwan to obtain high separation between the adsorbate and adsorbent. Dye's detection was carried out using a UV-VIS-T80-PG Ultraviolet-Visible (UV-Vis) spectrophotometer from Oasis Scientific Inc., UK. The X-ray diffraction (XRD) spectrometer of type XD3 from Persee/China and Fourier transform infrared (FTIR) spectrometer of type Spectrum Two N™ FT-NIR from PerkinElmer Waltham, MA/USA were used for characterization.

2.2.Adsorbate Solution

The initial solution, with a concentration of 1000 ppm for MB dye, was prepared by dissolving 1 g of the dye powder in 1 L of distilled water within a volumetric flask. Subsequent concentrations of the dye adsorbates were attained by diluting the stock solutions with distilled water. To achieve the desired pH levels, alkaline and acidic solutions were prepared using 0.1 M of NaOH and HCl diluted aqueous solutions. The pH of the solutions was adjusted using a calibrated pH meter (Mettler Toledo, Hamilton/New Zealand).

2.3.Adsorbent Preparation

After collecting the plant's inflorescence, they were washed with DI water to remove any possible dust and impurities. Then, acidic-nature water was used to rinse the collected inflorescence and clean it from any possible biological contaminations and microorganisms. Later, the plant was soaked and multiply washed with DI water to naturalize the plant; followed by heating at 60 °C in the oven for 12 h. The inflorescence tiny bristles were ground in a mill to minimize the size of the plant and screened with a 500 µm mesh. Finally, the product was dried again in the oven at 60 °C for 12 h and stored in a well-sealed container to avoid moisture. Figure 1 shows the preparation stages [20].

Fig. 1 Preparation of Adsorbent.

2.4.Batch Study Setup

The analysis in batches encompassed various parameters, including initial dye concentration (ranging from 5 to 50 mg/l), solution acidity levels (pH 3-11), the quantity of added PM (ranging from 0.1 to 2 g), contact time (5-180 min), and temperature variations (15-45 °C). This was done using an orbital shaker obtained from Stericox/India, at a speed of 150 rpm. For the pH adjustment, 0.1 M diluted NaOH and 0.1 M HCl solutions were employed. For the determination of the zero-charge point, the parameters were fixed at 30 minutes using DI water as the solvent, 0.2 g of the adsorbent, 50 mL of the sample, 25 °C, and 150 rpm. Generally, the data points were recorded at intervals until the equilibrium was obtained. The concentration of the dye was measured using a UV-Vis spectrophotometer at a fixed wavelength of 668 nm for MB dye under all conditions using a UV-9200 device obtained from Biotech Engineering Management Co. LTD. UK. The standard temperature and pH for operations were room temperature (RT) and 7, respectively. The removal efficiency and adsorption capacity (q_e) of MB were assessed following the methodology outlined by Kadhom et al. [21].

$$R\% = \frac{C_o - C_f}{C_o} x100\% \quad (1)$$

$$q_e = \frac{V(C_o - C_f)}{m} \quad (2)$$

where: C_o is the initial dye concentration in the feed-solution (mg/l), C_f is the final dye concentration after processing (mg/l), V is the aqueous solution volume (l), and m is the PM mass (g).

2.5.Kinetics Investigation

Adsorption kinetics provide significant understanding of the reaction pathways and interaction mechanisms between PM and the dye. The study examined the kinetic characteristics of the dye at a concentration of 20 mg/l under optimal conditions, specifically neutral pH, 150 rpm, 25 °C, and 0.5 g/50 ml of PM. The kinetics were explained by linear models of pseudo-first-order and pseudo-second-order kinetics. The rate of adsorption, according to pseudo-first-order kinetics, depends on the availability of adsorption sites, indicating a physical interaction between adsorbent and adsorbate, as seen in Equation 3 [20].

$$log(q_e - q_t) = log\, q_e - \frac{K_1}{2.303} t \quad (3)$$

In the context of adsorption kinetics, the variable t (in minutes) stands for time, and q_e and q_t stand for the amount of dye taken up at equilibrium and at a certain time, respectively, measured in mg/g. K_1 is a pseudo-first-order rate constant, which is measured in units of min^{-1}. According to the pseudo-second-order model, the adsorption rate is directly proportional to the square of the vacant sites, and site occupation is directly proportional to the adsorbate concentration. Additionally, it assumes a chemical interaction between the adsorbate and adsorbent; the model is shown in Equation 4 [20].

$$\frac{t}{q_t} = \frac{1}{K_2 q_e^2} + \frac{t}{q_e} \quad (4)$$

In this model, q_t and q_e (measured in mg/g) represent the adsorption capacity at any time and equilibrium, respectively. The variable t represents time in min, and K_2 is a pseudo-second-order constant, measured in g/mg min [22].

2.6.Isotherm Investigation

The adsorption equilibrium of MB was examined at various temperatures under optimal conditions using Langmuir and Freundlich isotherms as listed in equations 5 and 6, respectively [23].

$$\left[\frac{c_e}{q_e} = \frac{1}{K_L q_L} + \frac{c_e}{q_L}\right] \quad (5)$$

$$\left[\ln q_e = \ln K_F + \frac{1}{n_f} \ln c_e\right] \quad (6)$$

In these isotherms, C_e represents the equilibrium concentration of the dye in mg/l. q_e (measured in mg/g) represents the equilibrium dye uptake, and q_m (mg/g) represents the maximum uptake according to the Langmuir model. K_L is the Langmuir constant, measured in L/mg, while K_F is the Freundlich adsorption capacity, measured in $(mg/g)\times(mg/L)^{-1/n}$, and 1/n is the surface heterogeneity constant [24]. The Langmuir model postulates that adsorption results in a monolayer of molecules covering the surface of a homogeneous adsorbent. There is a limited number of comparable adsorption sites on the surface, each with the same adsorption energies. On the other hand, the Freundlich isotherm presupposes an adsorbent that is heterogeneous and has non-identical empty sites. It also suggests even heat dispersion over many layers of coverage [23].

2.7.Thermodynamic Investigation

Thermodynamic parameters were computed to study the impact of temperature on adsorption. The parameters discussed are the Gibbs free energy change (ΔG°), standard enthalpy change (ΔH°), and standard entropy change (ΔS°), calculated by the Van't Hoff equation [24, 25].

$$\Delta G° = -RTlnK \quad (7)$$

$$\Delta G° = \Delta H° - T\Delta S° \quad (8)$$

$$lnK = -\Delta H°/ RT + \Delta S°/R \quad (9)$$

$$K = C_{Ae}/C_{Se} \quad (10)$$

The symbol R represents the gas constant, which has a value of 8.314 J/mol·K. T denotes the temperature in °C, and K represents the equilibrium constant. Additionally, C_{Ae} and C_{Se} indicate the equilibrium concentrations of the dye on the PM and in the solution, respectively, both measured in mg/L. The activation energy was calculated via the Arrhenius equation [25].

$$lnK_2 = lnA - E/RT \quad (11)$$

where E represents the activation energy in J/mol, K_2 and A (measured in g/mol) are the

pseudo-second-order constant and Arrhenius constant, respectively.

2.8.Continuous System Setup

We also investigated the operation of PM in continuous mode adsorption, where a homemade fixed bed column was utilized for this case. Figure 2 shows a schematic diagram of the used system, in which four ports at a distance of 10 cm from each other were fixed into the column, generating four active areas of operation (we used only three). As the feed entered, the first zone was filled with inert sand. Then, the PM was packed within the second zone up to a height of 10 cm, while inert sand was filled in the third zone in the next 10 cm to hold the plant during operation. The final zone was left and no detection was recorded as no filling was used. The column contents were held by placing a 0.6 mm mesh at the ends of the column. The dimensions of the system and other operation conditions are listed in the figure below.

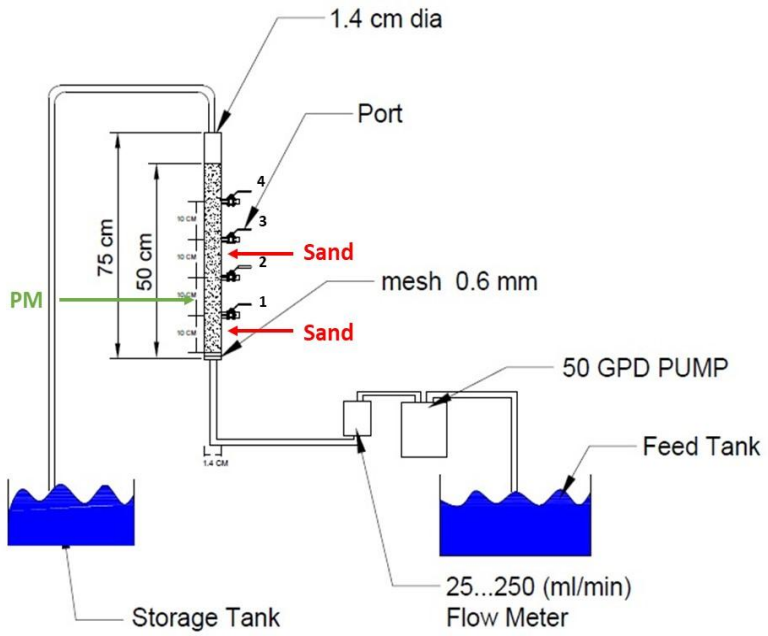

Fig. 2 A Homemade Fixed Bed System for Continuous Mode Adsorption.

3.RESULTS AND DISCUSSIONS

3.1.PM Characterizations

PM particles were characterized before and after the adsorption of 20 ppm dye. The XRD test was utilized to examine the structure of the adsorbent and the possible change in after adsorption. In the XRD setup, the angle (2θ) varies from 10 to 80 degrees with a precision of 0.01 degrees. XRD analysis is performed based on the detected peaks, where it was reported that a sharp peak indicates a crystalline structure, while the absence of a strong peak suggests an amorphous nature of the surface [26]. In our work, Figure 3 illustrates a representative XRD plot, revealing the amorphous characteristics of the PM. However, no change in the material's structure is detected after adsorption. From the figure, the main peak is observed at the angle of 23° in both cases; yet, small peaks in Figure 3b around 29.5, 61, and 74-76 could be referring to the presence of dye. Another characterization technique is the FTIR, where peaks of surface groups are detected and analyzed as presented in Figure 4. The obtained spectra indicated the existence of OH (hydrogen-bonded) based on a wide stretching absorption observed within the range of 3200-3550 cm^{-1}. The less intense –CH stretching bands are superimposed on the shoulder of the –OH band, namely in the spectral range of 2850 to 3000 cm^{-1}. The bands detected at around 2870 and 2960 cm^{-1} can be attributed to the stretching of -CH bonds. The presence of peaks in the range of 1630-1680 cm^{-1} indicates the presence of C=C bonds, which are characteristic of alkenes. However, the intensity of these peaks is lowered due to symmetry. The peaks observed at 1033-1091 cm^{-1} correspond to the presence of C-N bonds in amines [27]. By comparing the two figures, peaks around 1100, 1365, and 1620 cm^{-1} were detected that were assigned to S=O stretching, C=C side ring stretching, and C=N central ring stretching, respectively, appear after MB adsorption [28]. This could represent evidence for the adsorption occurrence.

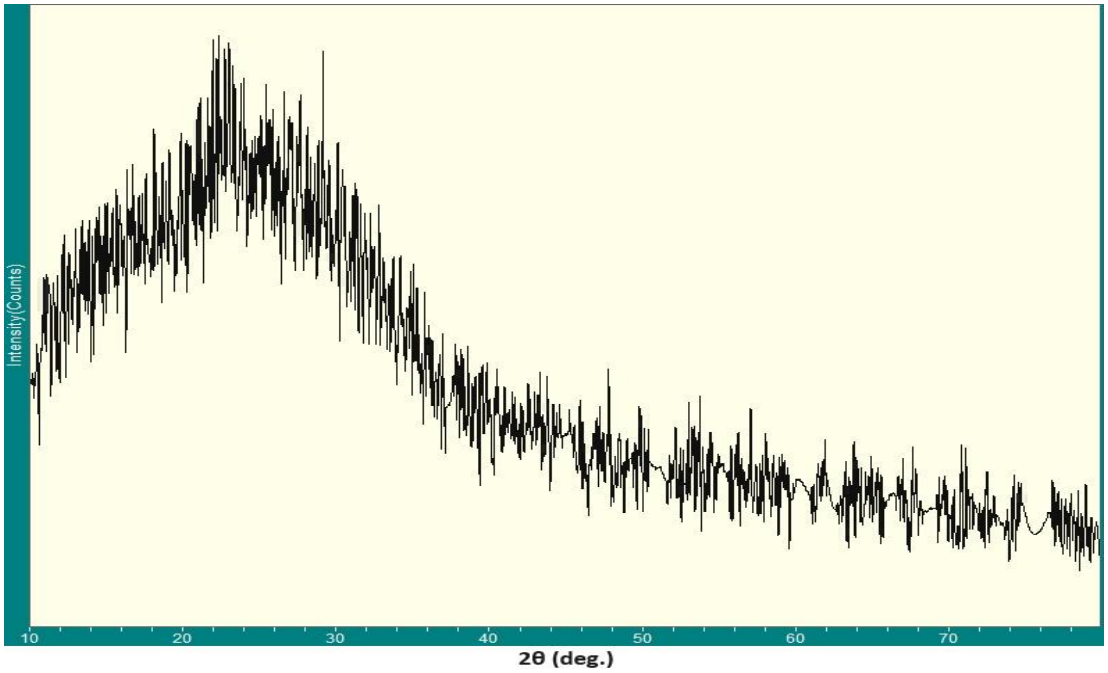

(a)

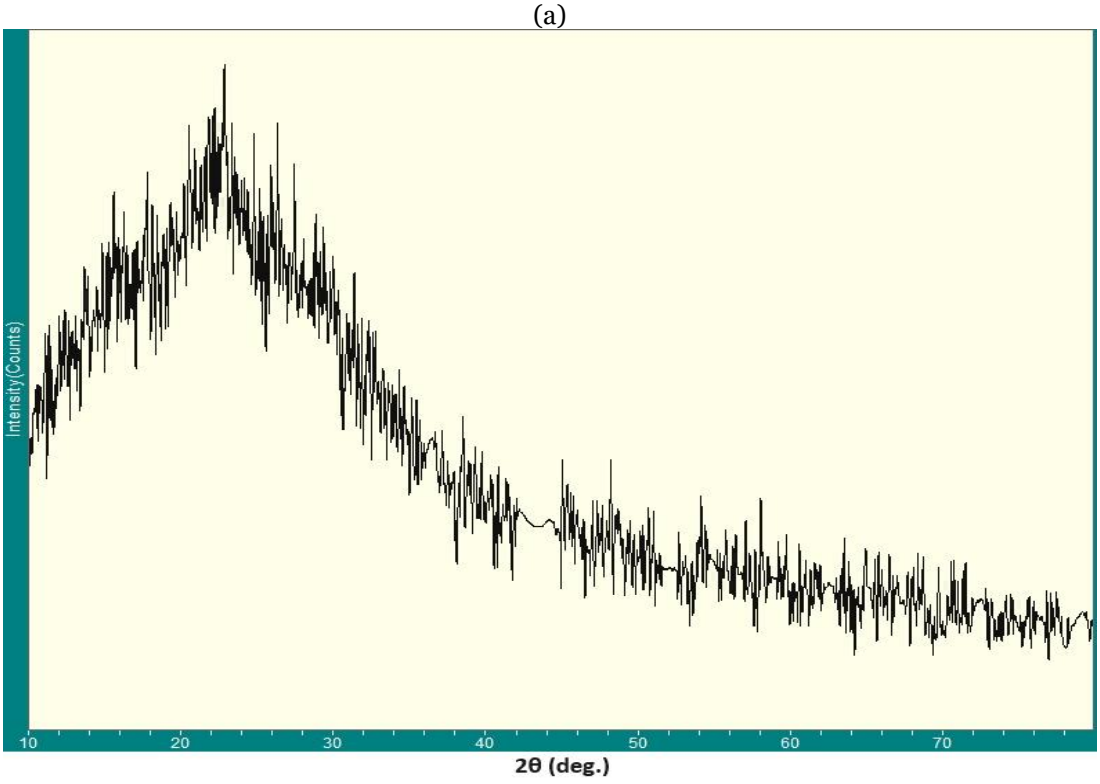

(b)

Fig. 3 XRD Test of the PM (a) Before and (b) After Adsorption of 20 ppm MB.

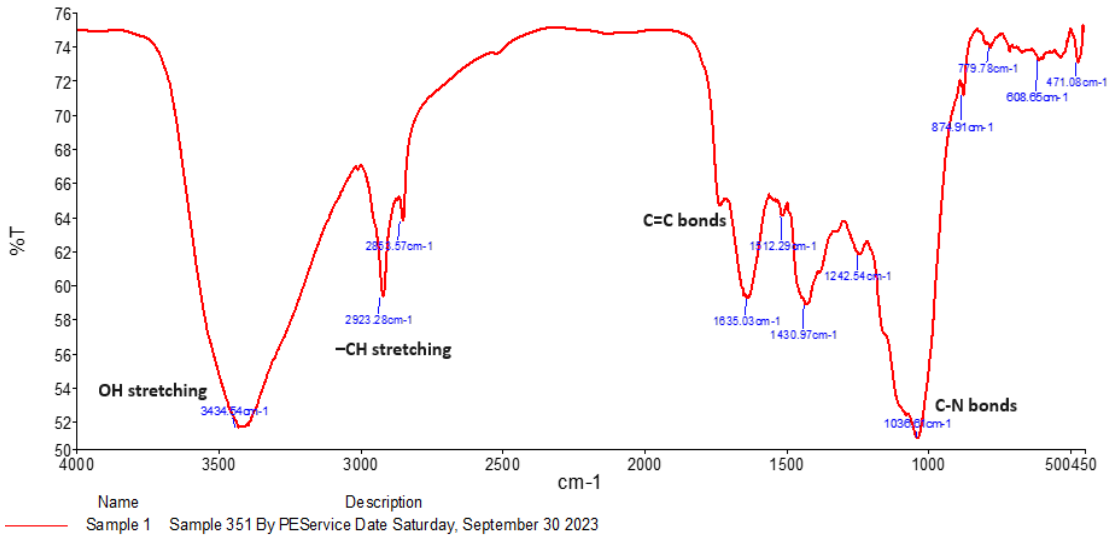

(a)

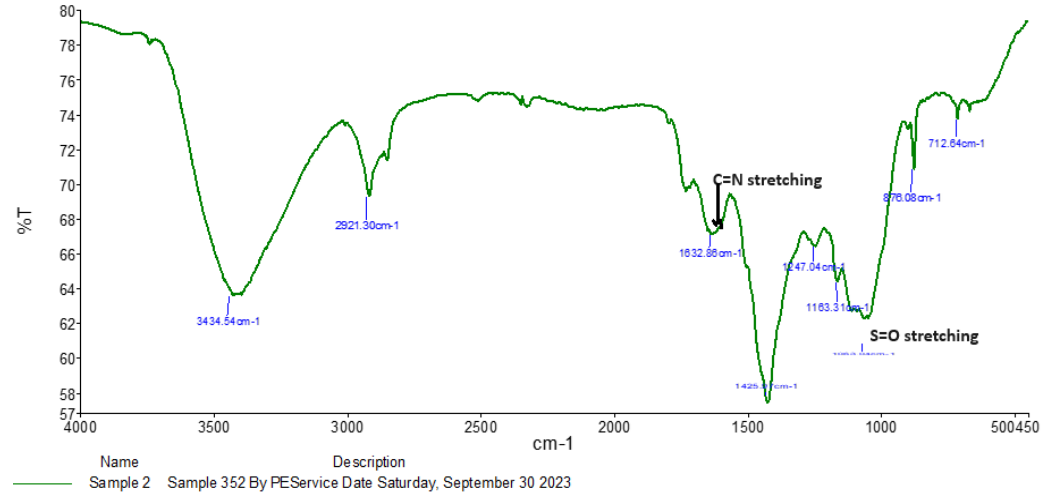

(b)

Fig. 4 FTIR Spectra for the PM (a) before and (b) after the Adsorption of 20 ppm MB.

3.2.Batch Mode: Operational Conditions Impact

The experimental section of our study investigated the impact of various physical parameters, including pH, point zero charge (PZC) pH, adsorbent dosage, dye concentration, contact time, and solution temperature, on the removal rate. The focus was primarily on identifying optimal operating conditions by analyzing the relationships between time, dye concentration, and adsorbent dosage. The standard adsorption curve and the specific results for each parameter are presented in the following sections.

3.2.1.Effect of pH

The study also sought to find out how the pH affects the removal of the dye, as it affects the dye as well as the adsorbent. The study was conducted with a focus on a range of pH from 3 to 11. To carry out the study, a series of solutions was prepared under the same conditions, except for the pH, which was adjusted to different values. These solutions, with a dye concentration of 30 mg/L, were agitated at 150 rpm and 25 °C for 30 min using 0.2 g of adsorbent per 50 ml of solution. The pH variations revealed noticeable alterations in dye removal rates. Figure 5 illustrates the influence of the solution's pH on the rate of dye removal at pH values of 3, 5, 7, 9, and 11. The results indicate that the rate of removing the dye is low at a low pH of 3, which is a consequence of the acidic nature of the solution, as discussed in the introduction. At a low pH, the surface of the adsorbent carries a positive charge, which causes electrostatic repulsion with the cationic dye as well as the positive ions in the solution, as noted in another study [29]. The maximum rate of removing the dye is achieved at a pH of 7, with a reduction in the rate at a high pH. As the MB loses a proton to become deprotonated, thus carrying a negative charge, which causes electrostatic repulsion with the negatively charged surface. Here, the rate of removing the anionic dye molecules is reduced, which was

previously detected in another study [30]. The optimal rate of removing the dye is achieved at a near-neutral solution, as the electrostatic forces are minimized, thus reducing the interaction between the dye molecules and the surface, as noted in another study. The rate of removing the dye is rapid, reaching up to 78% of the equilibrium capacity.

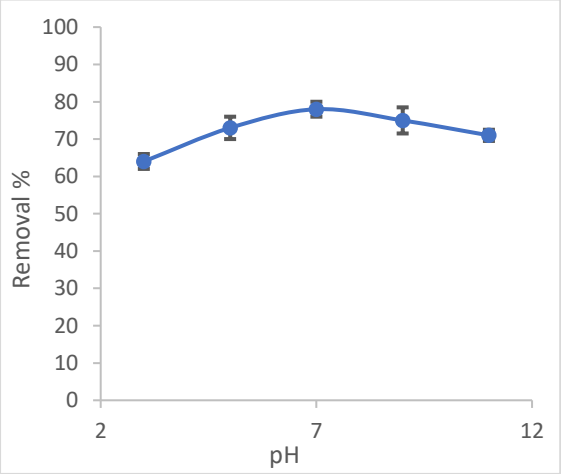

Fig. 5 Effect of pH on MB Adsorption on the PM.

3.2.2.PZC Measurement

The PZC is the pH level at which the surface of a material becomes neutral in terms of electricity. It is very important for studying colloidal systems because it could affect the adsorption and ion exchange. When the pH is below the PZC, the surface has a positive charge, and when it is above the PZC, it has a negative charge. On the other hand, an alkaline PZC means that the surface is negatively charged at the pH until the PZC is reached [31]. Figure 6 illustrates the PZC by plotting the difference between the final pH and initial pH against the initial pH. The graph indicates that the PZC is detected at an initial pH of 6.2, which is somewhat natural. Hence, below this pH, the material's surface carries a positive charge, and vice versa. By comparing Figure 6 with the obtained information from Figure 5, the findings refer to similar behavior.

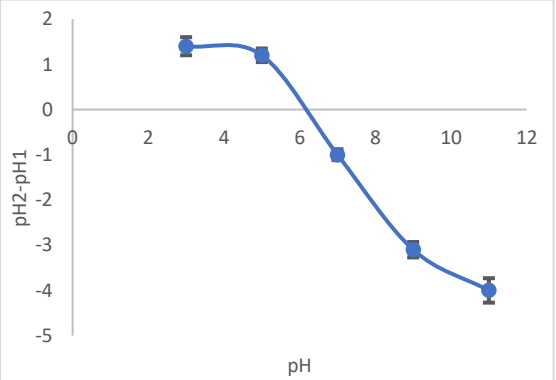

Fig. 6 PZC of PM.

3.2.3.Dose Effect

To investigate the impact of the adsorbent on the adsorption process, various quantities of PM ranging from 0.1 to 2 g were utilized in a sample volume of 50 ml. The experiments were conducted at 25 °C with a mixing speed of 150 rpm while maintaining the dye concentration at 30 ppm and natural pH. Figure 7 illustrates the influence on removal rates after 30 min contact time. While a dose of 0.5 g gave an 82% rate, the lowest dose gave a 62% rate. The boost comes from the more available empty sites, which are well distributed, thus increasing the surface area for exposure. However, if more adsorbents are used, they might stick together, thereby reducing their surface area, which in turn will reduce the rate of removal [32,33].

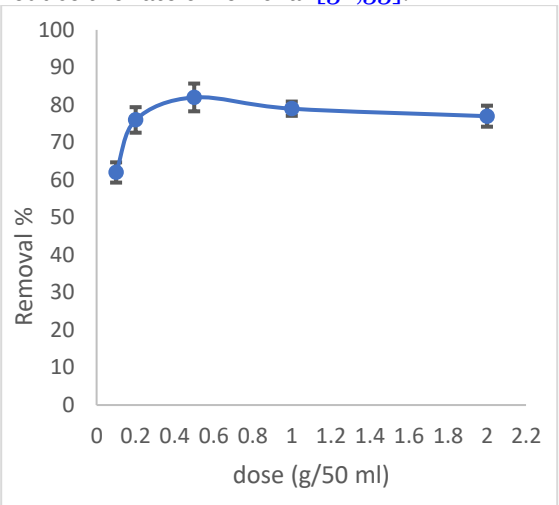

Fig. 7 Effect of Dose on MB Removal Rate.

3.2.4.Initial Concentration

The initial dye concentration is an important factor in adsorption, while the sorbent's capacity remains constant. In other words, the process of adsorption depends on the concentration of the dye. Our study covered a range of dye's concentrations from 5 to 50 mg/L. The study maintained constant conditions such as 0.5 g of PM, 50 ml of the dye solution, 30 minutes of time, 150 rpm of stirring speed, 25 °C, and pH at neutral levels. As illustrated in Figure 8, the rate of dye removal increased with concentration, reaching a maximum of 85 % at 20 mg/L. However, a reduction in the removal rate was observed beyond this point. For example, when a 5 ppm dye-aqueous solution was used, the removal rate was 48%. In contrast, using a 50 ppm solution resulted in a removal rate of 71%. Research suggests that lower initial dye concentrations lead to increased removal rates due to the availability of more vacant binding sites, allowing for efficient and rapid adsorption. In contrast, higher dye concentrations may result in molecules competing for accessible sites, leading to saturation and reduced removal effectiveness. Under typical conditions, the capacity of PM particles increases until all initial vacant binding sites are filled with dye, after which the adsorption rate slows down as the sites become more saturated [34, 35].

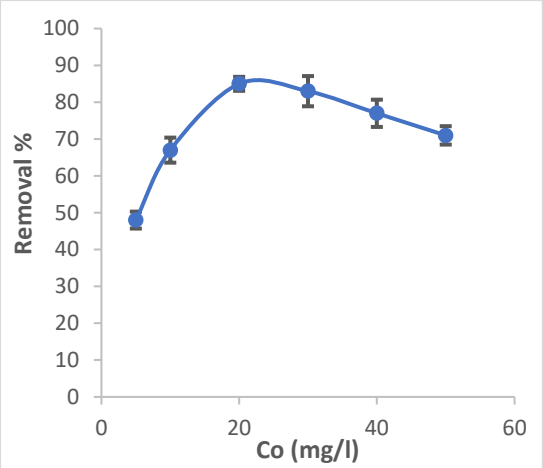

Fig. 8 Effect of Dye's Initial Concentration on Removal Rate.

3.2.5.Contact Time Effect

The adsorption time was studied to identify the optimum time of operation as presented in Figure 9. At first, as the contact time increased, the removal ratio increased sharply. After 30 min of mixing, the removal rate reached 82%. However, the increase in removal rate was marginal as the time elongated, indicating a state of partial equilibrium. It is noticed that after 120 min of mixing, the removal rate reached 93%. Yet, this enhancement is considered negligible in terms of the relatively long consumed time. The increase in R% was initially sharp due to the available adsorption sites on the adsorbent's surface. As the sites are occupied, no further sites are available to uptake the left dye, where the equilibrium state is obtained [36]. As the time is investigated, the other parameters were fixed as follows: PM dose= 0.5 g, sample volume= 50 ml, pH= 7, initial dye concentration= 20 ppm, mixing rate= 150 rpm, and temperature= 25 °C.

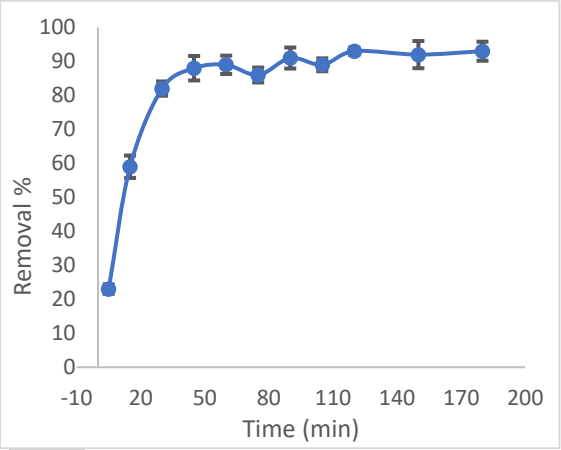

Fig. 9 Effect of Contact Time on the Removal Rate of MB.

3.2.6.Temperature Effect

The investigation analyzed the impact of different solution temperatures (15, 25, 35, and 45 °C) on the removal rate while keeping all other factors constant. These factors included a dye concentration of 20 ppm, solution volume of 50 ml, mixing speed of 150 rpm, contact period of 60 min, natural pH, and adsorbent dosage of 0.5 gm. Here, Figure 10 illustrates the influence of varying temperatures on removal rate. The graph depicts a slight increase in the tested removal as the temperature increased, where the removal rate increased from 81% to 87% at temperatures of 15 and 45 °C, respectively. The findings suggest that the process does not significantly involve heat absorption or release, although it tends to be endothermic in nature. This could be explained as higher temperatures typically enhance the bonding forces between the adsorbed substance and the adsorbent material [37].

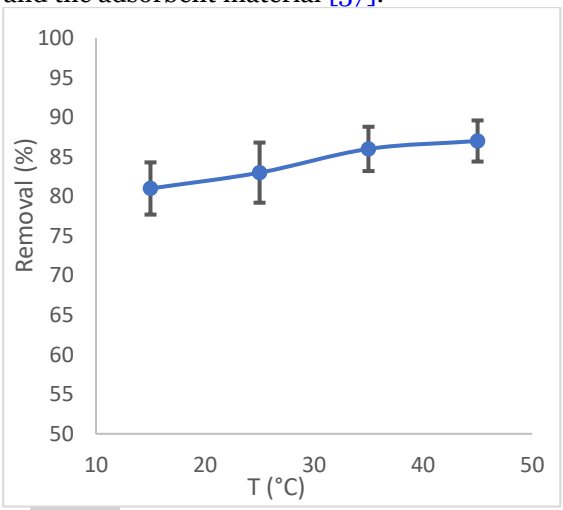

Fig. 10 Effect of Temperature on Removal Rate.

3.3.Fixed Bed Mode: Operational Conditions Impact

3.3.1.Effect of Flow Rate

Using the continuous flow system, the impact of flow rate (Q) on the removal efficiency was investigated by operating at three different flow rates: 75, 125, and 200 ml/min. As described in section 2-8, the active static height was 10 cm that was filled with the PM. The below and above regions of the column, of heights of 10 cm each, were filled with inert sand, so no noticeable effect is considered. At the beginning of each section, a prob was set to monitor the results. Figure 11 shows the effect of Q on the removal rates measured from three ports. The other parameters were fixed; here, the velocity was 0.122 m/min and the initial concentration was 20 ppm of MB. As port 1 is placed at the entrance of the PM section, it maintained almost zero throughout the whole operation, as the used sand as a stabilizing layer is inert. Also, the reads of ports 2 and 3 are almost identical because port 2 is placed at the end of PM layer, while port 3 is after the second inert sand layer that has no contribution to the operation. When the operation was started, the removal rate was almost full, which is attributed to the availability of adsorption sites, where the removal rates were measured from the initial concentration of the feed and the concentration of the output liquid after being in contact with the adsorbent. From the figure, the removal

rate reached o in a short operating time as the Q increased. This is attributed to the faster occupation of dye molecules within the adsorbent. Also, the curve decreased sharper as the Q raised up for the same reason [38].

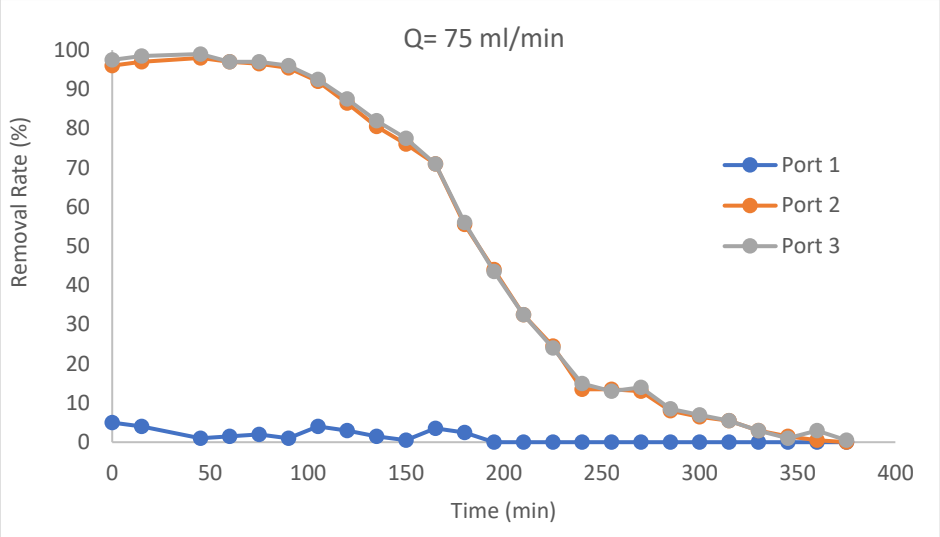

(a)

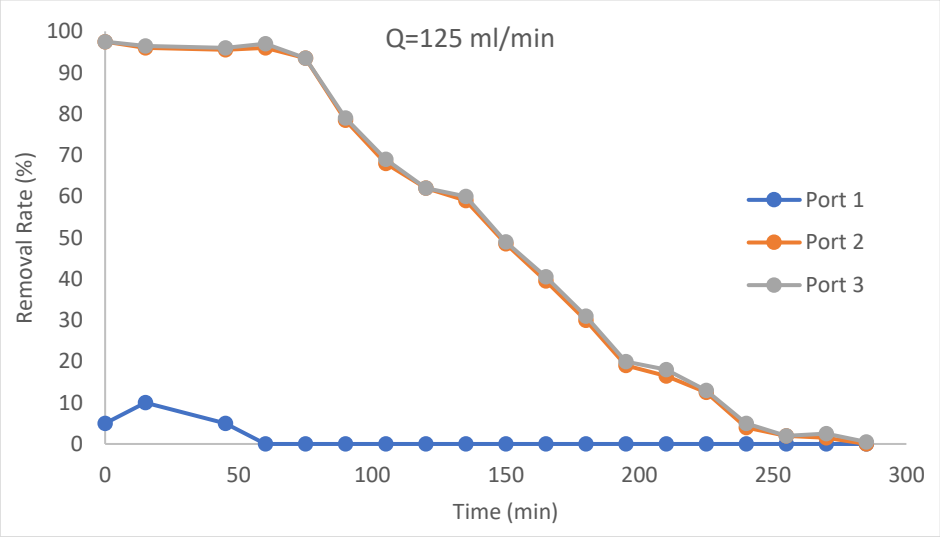

(b)

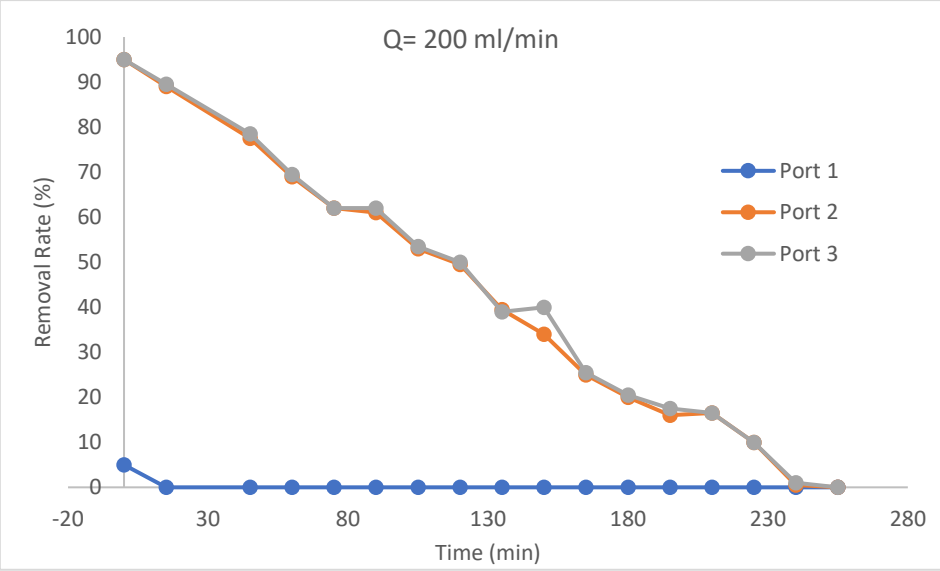

(c)

Fig. 11 Effect of Operating Flow Rate on the Removal Efficiency.

3.3.2.Effect of Iinitial Concentration

In order to investigate the effect of concentration, the initial concentration was increased from 20 ppm (illustrated in Figure 11 (a)) to 30 ppm (Figure 12) while keeping the same other operational conditions, mainly the Q= 75 l/min. In Figure 12, we can observe that the removal reached its maximum capacity within 285 min. This could be explained as the concentration of the dye increases, the adsorption sites are faster occupied and reach their maximum [39].

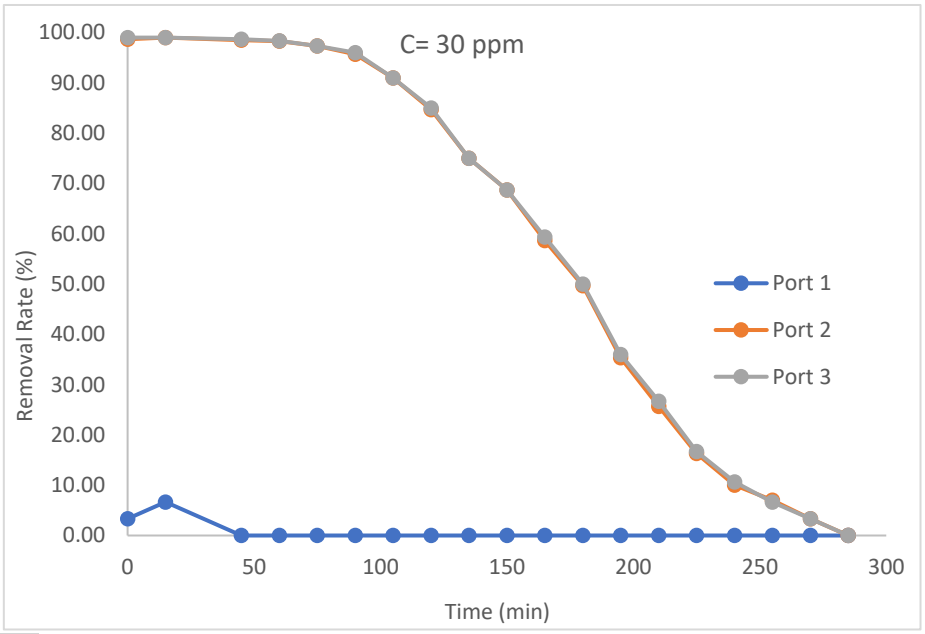

Fig. 12 Effect of Time on Removal Rate Employing an Initial Concentration of 30 ppm.

3.3.3.Effect of Column Height

The static height of the fixed bed column was manipulated to optimize the operation conditions. Using a flow rate of 75 ml/min and the same other conditions described in section 3-3-1 of Figure 11(a) case, the system was operated using a packed PM of height 5 cm instead of 10 cm. Findings are illustrated in Figure 13, where shorter operational time is obtained. This observation is clarified as the amount of adsorbent is larger in the 10 cm column, which gives a longer operation.

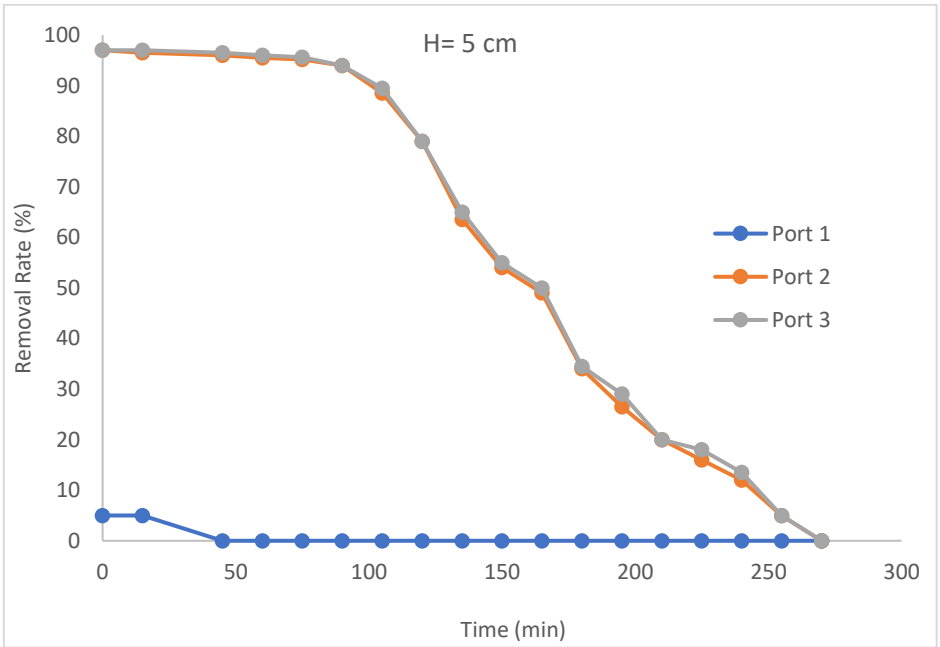

Fig. 13 The Effect of Time on the Removal Rate Using a 5 cm Height Fixed Bed Column.

3.4.Theoretical Calculations

3.4.1.Kinetics Study

Understanding adsorption kinetics is pivotal for grasping the mechanism and speed of the adsorption process. We have selected two commonly used models, pseudo-first-order and pseudo-second-order, each is based on different assumptions. We computed the R^2

value for each model to assess its correspondence with the experimental data and determine the most suitable model. The R^2 values for the different kinetic models were 0.818 and 0.993 for the pseudo-first-order and pseudo-second-order, respectively. As the findings align with the pseudo-second-order model, it is suggested that the adsorption rate is unaffected by concentration and is governed by adsorption capacity. This model considers the potential limitation of chemisorption rate on adsorption, which could stem from the number of surface groups. The pseudo-second-order model accurately predicts the equilibrium adsorption capacity, as evidenced by Sahoo and Prelot [40]. Figure 14 depicts the connections between the models' calculations.

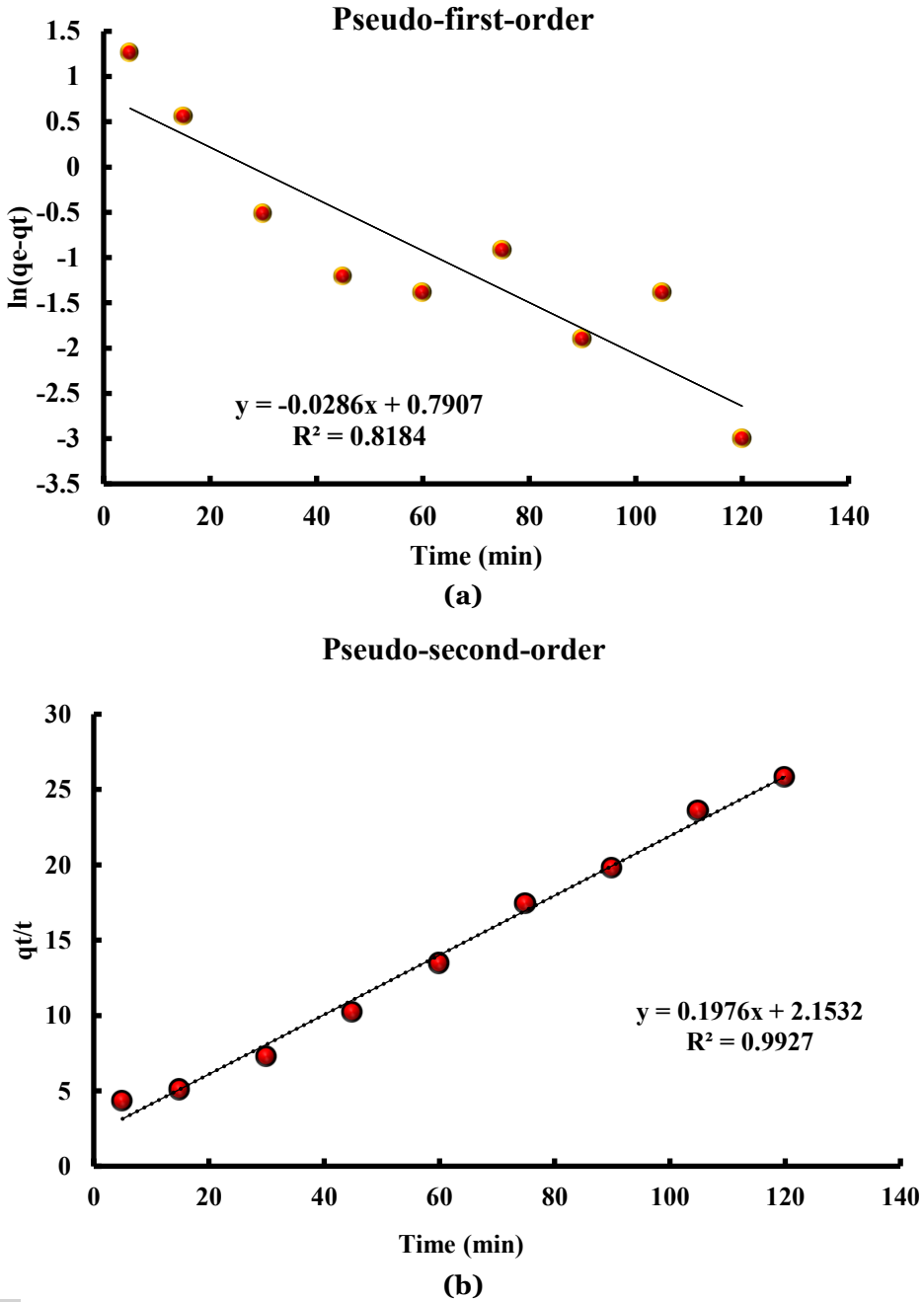

Fig. 14 Kinetics Study Using (a) Pseudo First Order and (b) Pseudo Second Order Models.

3.4.2.Isotherms Study

Studying isotherms is crucial for comprehending the interplay between the adsorbent and adsorbate in the adsorption process. Certain models are commonly employed due to their compatibility with experimental data. We applied the Langmuir and Freundlich isotherms, which are the most well-known ones, in our research. Real-world data with predictions from theoretical models were compared to find the best model. The model with the highest coefficient of determination (R^2) clearly explained how adsorption works [41]. Nonetheless, the comprehensive equations and parameter definitions are delineated in our preceding study [21]. In Figure 15, you can see the two models. The R^2 values for the Langmuir and

Freundlich models were 09592 and 0.9865, respectively. The results are consistent with the Freundlich model, indicating that the adsorption rate is independent of concentration and is exclusively influenced by adsorption capacity. Yet, the maximum adsorption capacity was 20.2 mg/g. This model accommodates the potential constraint of chemisorption rate on adsorption, which could arise from the number of surface groups [40]. It is good to mention that the b and R_L values of Langmuir model at the maximum adsorption were 0.08283 and 0.707, respectively, while K_f of Freundlich model was 1.7516.

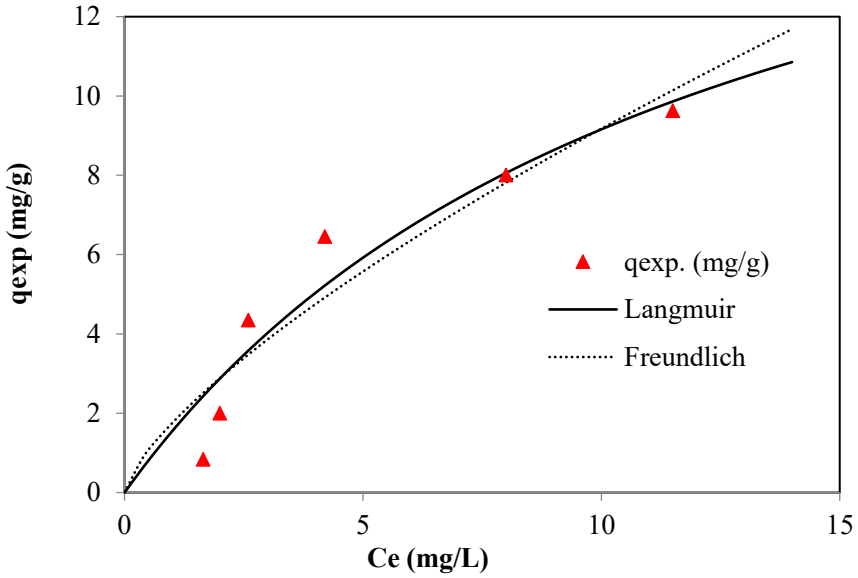

Fig. 15 The Isotherm Models: Langmuir and Freundlich.

3.4.3.Thermodynamic Studies

The standard enthalpy change (ΔH^o) and standard entropy change (ΔS^o) can be determined by analyzing the slope and intercept of the Van't Hoff equation, as presented in Table 1. To obtain these calculations, a plot of $\ln K_c$ against 1/T is employed [24]. The negative value of Gibbs free energy (ΔG^o) in Table 1 indicates a spontaneous and feasible adsorption process. Moreover, as the temperature rises, the ΔG^o value decreases. This decrease suggests that the increased mobility of molecules at higher temperatures makes adsorption more favorable; our findings in Figure 10 support this observation [42]. The positive enthalpy value implies an endothermic reaction, which also supports our findings. Furthermore, the positive entropy value denotes an increase in unpredictability at the interface [43]. In order to present the performance of the used adsorbent (PM), we compared it with other works that used biomass waste in Table 2.

Table 1 Thermodynamic Parameters.

Temp. (K)	K_c	ΔG^o (KJ/mol)	ΔH^o (KJ/ mol)	ΔS^o (J /mole.K)
288	1.4138	-0.8292		
298	1.6743	-1.2769	12.0661082	44.775047
308	1.9611	-1.7246		
318	2.2743	-2.1725		

Table 2 A Performance Comparison of different Biomass-Based Adsorbents to Adsorb MB.

Adsorbent	Adsorption Capacity (mg/g)	Reference
Polypogon monspeliensis	20.2	This work
Walnut Shell	19.99	[44]
peroxide-treated rice husk	18.7	[45]
nitric acid-treated peanut shell	18.5	[45]
nitric acidtreated rice husk	14.1	[45]
peroxide-treated peanut shell	18.2	[45]
Gundelia seeds waste	30.57	[20]
Wheat shells	4.2	[46]
activated banana peel	19.67	[47]

4.CONCLUSIONS

This study explored the use of Polypogon monspeliensis to adsorb MB dye from simulated wastewater as a cost-free, sustainable, simply prepared, and ecofriendly adsorbent. The study included the use of batch and continuous modes, where the common affective factors are investigated. In the batch system, the ideal operational settings were found to be neutral pH, moderate adsorbent dose (0.5 g/50 ml), lower dye concentrations, and 30 min of contact time. It was found that the PM was highly effective at removal, with removal percentages exceeding 80 % under various conditions, indicating good adsorption properties. The kinetics showed that the process was pseudo-second-order, indicating chemisorption, and the isotherm fits showed good agreement with both Langmuir and Freundlich isotherms, but the Freundlich model was preferred. The thermodynamics showed that the process was spontaneous and endothermic, and that the amount of adsorption increased with an increase in temperature. In continuous mode, the removal of MB was dependent on flow rate, initial concentration of dye, and column height. The removal percentages for 90 minutes at 10 cm and 5 cm column heights at a flow rate of 75 mL/min and an initial concentration of 20 ppm were 96% and 94%, respectively. Future studies may include the optimization of operating parameters for better efficiency and the application of PM in wastewater treatment. Future studies may include the regeneration and reuse of the material and its ability to remove more contaminants from wastewater.

ACKNOWLEDGMENT

The authors like to thank the Department of Environmental Science at the Alkarkh University of Science for partially supporting this work.

FUNDING

No Funds were received.

CONFLICT OF INTEREST

The authors declare no known conflict for this work.

REFERENCES

[1] Ahmed AU, Ibraheem H, Kadhom M, Rashad AA, Al-Dahhan WH, Bufaroosha M, et al. **Modified PVC as Adsorbent for Methyl Orange Dye Removable.** *AIP Conference Proceedings* 2022; **2398**(1): 020006.

[2] Ismail Z, Go YI. **Fog-to-Water for Water Scarcity in Climate-Change Hazards Hotspots: Pilot Study in Southeast Asia.** *Global Challenges* 2021; **5**(4): 2000036.

[3] Droogers P, Immerzeel WW, Terink W, Hoogeveen J, Bierkens MFP, van Beek LPH, et al. **Water Resources Trends in Middle East and North Africa Towards 2050.** *Hydrology and Earth System Sciences* 2012; **16**: 3101–3114.

[4] Karadag D, Akgul E, Tok S, Erturk F, Kaya MA, Turan M. **Basic and Reactive Dye Removal Using Natural and Modified Zeolites.** *Journal of Chemical & Engineering Data* 2007; **52**(6): 2436–2441.

[5] Silva F, Nascimento L, Brito M, da Silva K, Paschoal W, Fujiyama R. **Biosorption of Methylene Blue Dye Using Natural Biosorbents Made from Weeds.** *Materials* 2019; **12**(15): 2486.

[6] Küçükosmanoğlu M, Gezici O, Ayar A. **The Adsorption Behaviors of Methylene Blue and Methyl Orange in a Diaminoethane Sporopollenin-Mediated Column System.** *Separation and Purification Technology* 2006; **52**(2): 280–287.

[7] Salih SS, Mohammed HN, Abdullah GH, Kadhom M, Ghosh TK. **Simultaneous Removal of Cu(II), Cd(II), and Industrial Dye onto a Composite Chitosan Biosorbent.** *Journal of Polymers and the Environment* 2020; **28**: 354–365.

[8] Salih SS, Mahdi A, Kadhom M, Ghosh TK. **Competitive Adsorption of As(III) and As(V) onto Chitosan/Diatomaceous Earth Adsorbent.** *Journal of Environmental Chemical Engineering* 2019; **7**(3): 103407.

[9] Jawad AH, Kadhum AM, Ngoh YS. **Applicability of Dragon Fruit (Hylocereus polyrhizus) Peels as Low-Cost Biosorbent for Adsorption of Methylene Blue from Aqueous Solution: Kinetics, Equilibrium and Thermodynamics Studies.** *Desalination and Water Treatment* 2018; **109**: 231–240.

[10] Adil H, Hussain Z, Kadhom M, Yousif E. **Adsorptive Removal of Safranin-O Dye from Aqueous Solutions Using Carrot Seed.** *AIP Conference Proceedings* 2022; **2386**(1): 040011.

[11] Salih SS, Kadhom M, Shihab MA, Ghosh TK. **Competitive Adsorption of Pb(II) and Phenol onto Modified Chitosan/Vermiculite Adsorbents.** *Journal of Polymers and the Environment* 2022; **30**: 4238–4251.

[12] Boakye P, Ohemeng-Boahen G, Darkwah L, Sokama-Neuyam YA, Appiah-Effah E, Oduro-Kwarteng S, et al. **Waste Biomass and Biomaterials Adsorbents for Wastewater Treatment.** *Green Energy and Environmental Technology* 2022; **2022**: 1–25.

[13] Moussavi G, Mahmoudi M. **Removal of Azo and Anthraquinone Reactive**

Dyes from Industrial Wastewaters Using MgO Nanoparticles. *Journal of Hazardous Materials* 2009; **168**(2-3): 806–812.

[14] Alalwan HA, Kadhom MA, Alminshid AH. **Removal of Heavy Metals from Wastewater Using Agricultural Byproducts.** *Journal of Water Supply: Research and Technology - AQUA* 2020; **69**(2): 99–112.

[15] Kadhom M, Albayati N, Alalwan H, Al-Furaiji M. **Removal of Dyes by Agricultural Waste.** *Sustainable Chemistry and Pharmacy* 2020; **16**: 100259.

[16] Duan F, Zhu Y, Yu H, Wang A. **Facile Fabrication of the Porous Adsorbent from Natural Plant Angelica Sinensis Stabilized Liquid Foam for Dye Removal.** *Green Chemical Engineering* 2022; **3**(1): 83–91.

[17] Duan F, Zhu Y, Yu H, Wang A. **Porous Materials Fabricated from Pickering Foams Stabilized by Natural Plant of Angelica sinensis for Removal of Cd (II) and Cu (II).** *Colloids and Surfaces A: Physicochemical and Engineering Aspects* 2022; **648**: 128695.

[18] Abbasi A, Khatoon F, Ikram S. **A Review on Remediation of Dye Adulterated System by Ecologically Innocuous "Biopolymers/Natural Gums-Based Composites."** *International Journal of Biological Macromolecules* 2023; **231**: 123240.

[19] Kaur N, Kaushal J, Mahajan P. **Phytoremediation Potential of Hibiscus rosa-sinesis for Removal of Methylene Blue Dye and its Kinetic, Adsorption Studies in Aquatic System.** *Asian Journal of Chemistry* 2022; **34**(10): 2710–2716.

[20] Albayati N, Mohammed M, Ahmed H, Kadhom M. **The Potential of Gundelia Seeds Waste as an Emerging Sustainable Adsorbent for Methylene Blue-Polluted Water Treatment.** *Progress in Color, Colorants and Coatings* 2024; **17**(3): 243–256.

[21] Kadhom M, Kalash K, Al-Furaiji M. **Performance of 2D MXene as an adsorbent for malachite green removal.** *Chemosphere* 2022; **290**: 133256.

[22] Mahmood OAA-Q, Waisi BI. **Crystal Violet Dye Removal from Aqueous Water Using Polyacrylonitrile Precursor Beads.** *Materials Today: Proceedings* 2021; **42**: 2185–2192.

[23] Al-Jubouri SM, Al-Jendeel HA, Rashid SA, Al-Batty S. **Green synthesis of porous carbon cross-linked Y zeolite nanocrystals material and its performance for adsorptive removal of a methyl violet dye from water.** *Microporous and Mesoporous Materials* 2023; **356**: 112587.

[24] Du C, Song Y, Shi S, Jiang B, Yang J, Xiao S. **Preparation and characterization of a novel Fe3O4-graphene-biochar composite for crystal violet adsorption.** *Science of The Total Environment* 2020; **711**: 134662.

[25] Handbook of Nanomaterials for Wastewater Treatment. **Elsevier**; 2021.

[26] Mahmood Ansari T, Asif Hanif M, Umbreen K, Nadeem R. **Polypogon monspeliensis Waste Biomass: A Potential Biosorbent for Cd (II).** *African Journal of Biotechnology* 2009; **8**(7): 1136–1142.

[27] Manea YK, Khan AM. **Enhanced Photocatalytic Degradation of Methylene Blue and Adsorption of Metal Ions by SDS-TiP Nanocomposite.** *SN Applied Sciences* 2019; **1**: 821.

[28] Kumar R, Ahmad R. **Biosorption of Hazardous Crystal Violet Dye from Aqueous Solution onto Treated Ginger Waste (TGW).** *Desalination* 2011; **265**(1): 112–118.

[29] Shamsipur M, Barati A, Nematifar Z. **Fluorescent pH Nanosensors: Design Strategies and Applications.** *Journal of Photochemistry and Photobiology C: Photochemistry Reviews* 2019; **39**: 76–141.

[30] Luo H, Liu Y, Lu H, Fang Q, Rong H. **Efficient Adsorption of Tetracycline from Aqueous Solutions by Modified Alginate Beads after the Removal of Cu(II) Ions.** *ACS Omega* 2021; **6**(9): 6240–6251.

[31] Singh P, Sarswat A, Pittman CU, Mlsna T, Mohan D. **Sustainable Low-Concentration Arsenite [As(III)] Removal in Single and Multicomponent Systems Using Hybrid Iron Oxide–Biochar Nanocomposite Adsorbents—A Mechanistic Study.** *ACS Omega* 2020; **5**(6): 2575–2593.

[32] Zhou G, Wang KP, Liu HW, Wang L, Xiao XF, Dou DD, et al. **Three-dimensional polylactic acid@graphene oxide/chitosan sponge bionic filter: Highly efficient adsorption of crystal violet dye.** *International Journal of Biological Macromolecules* 2018; **113**: 792–803.

[33] S R, Lata S, P B. **Biosorption characteristics of methylene blue and malachite green from simulated wastewater onto Carica papaya wood biosorbent.** *Surfaces and Interfaces* 2018; **10**: 197–215.

[34] Oladoye PO, Kadhom M, Khan I, Hama Aziz KH, Alli YA. **Advancements in adsorption and photodegradation technologies for Rhodamine B dye wastewater treatment: fundamentals, applications, and future directions.** *Green Chemical Engineering* 2023; **5**(1): 12–30.

[35] Boudrahem F, Aissani-Benissad F, Soualah A. **Removal of basic yellow dye from aqueous solutions by sorption onto reed as an adsorbent.** *Desalination and Water Treatment* 2014; **54**(9): 1–8.

[36] Salih SS, Shihab MA, Mohammed HN, Kadhom M, Albayati N, Ghosh TK. **Chitosan-vermiculite Composite Adsorbent: Preparation, Characterization, and Competitive Adsorption of Cu(II) and Cd(II) Ions.** *Journal of Water Process Engineering* 2024; **59**: 105044.

[37] Sahoo TR, Prelot B. **Adsorption Processes for the Removal of Contaminants from Wastewater.** *Nanomaterials for the Detection and Removal of Wastewater Pollutants*, Elsevier; 2020, p. 161–222.

[38] Azeez NR, Salih SS, Kadhom M, Mohammed HN, Ghosh TK. **Enhanced Termination of Zinc and Cadmium Ions from Wastewater Employing Plain and Chitosan-Modified Mxenes: Synthesis, Characterization, and Adsorption Performance.** *Green Chemical Engineering* 2023; **5**(1): 45–58.

[39] Laskar N, Kumar U. **Adsorption of Crystal Violet from Wastewater by Modified Bambusa Tulda.** *KSCE Journal of Civil Engineering* 2018; **22**: 2755–2763.

[40] Saad M, Tahir H, Khan J, Hameed U, Saud A. **Synthesis of Polyaniline Nanoparticles and Their Application for the Removal of Crystal Violet Dye by Ultrasonicated Adsorption Process Based on Response Surface Methodology.** *Ultrasonics Sonochemistry* 2017; **34**: 600–608.

[41] Farch S, Yahoum MM, Toumi S, Tahraoui H, Lefnaoui S, Kebir M, et al. **Application of Walnut Shell Biowaste as an Inexpensive Adsorbent for Methylene Blue Dye: Isotherms, Kinetics, Thermodynamics, and Modeling.** *Separations* 2023; **10**(1): 60.

[42] Manoj Kumar Reddy P, Mahammadunnisa Sk, Ramaraju B, Sreedhar B, Subrahmanyam Ch. **Low-Cost Adsorbents from Bio-Waste for the Removal of Dyes from Aqueous Solution.** *Environmental Science and Pollution Research* 2013; **20**: 4111–4124.

[43] Banerjee S, Chattopadhyaya MC, Uma, Sharma YC. **Adsorption Characteristics of Modified Wheat Husk for the Removal of a Toxic Dye, Methylene Blue, from Aqueous Solutions.** *Journal of Hazardous, Toxic, and Radioactive Waste* 2014; **18**(1): 56–63.

[44] Amela K, Hassen MA, Kerroum D. **Isotherm and Kinetics Study of Biosorption of Cationic Dye onto Banana Peel.** *Energy Procedia* 2012; **19**: 286–295.